Tungsten-containing MCF silica as active and recyclable catalysts for liquid-phase oxidation of 1, 3-butanediol to 4-hydroxy-2-butanone

Yang Su, Yong-Mei Liu, Lu-Cun Wang, Miao Chen, Yong Cao[*], Wei-Lin Dai, He-Yong He, Kang-Nian Fan[**]

Department of Chemistry, Shanghai Key Laboratory of Molecular Catalysis and Innovative Materials, Fudan University, Shanghai 200433, PR China

Abstract

W-containing mesocellular silica foams (MCF) having a Si/W (molar) ratio of 10–40 were synthesized and characterized by means of N_2 adsorption, SAXS, XRD, TEM, DRIFTS, DR UV–vis and Raman spectroscopy. The results show that tungsten was well incorporated inside the MCF material and the nature of WO_x species closely depends on the tungsten content. At low tungsten content (Si/W ≥ 20), the characteristic mesocellular structure of the MCF material was well maintained while at higher tungsten content (Si/W ∼ 10) a significant degradation of the mesocellular arrangement of MCF pores was observed. The selective liquid-phase oxidation of 1,3-butanediol (1,3-BDO) to 4-hydroxy-2-butanone (HB) over the W-MCF material with various Si/W ratios was investigated. Under optimized reaction conditions, the W-MCF catalyst showed a superior catalytic performance in the selective oxidation of 1,3-BDO as compared to other W-containing materials such as WO_3/MCF and W-SBA-15. Moreover, a very stable catalytic activity as a function of cycling test was observed for the W-MCF catalyst.
© 2006 Elsevier B.V. All rights reserved.

Keywords: Tungsten; Mesocellular silica foams (MCF); 4-Hydroxy-2-butanone (HB); 1,3-Butanediol (1,3-BDO); Hydrogen peroxide; Liquid-phase oxidation

1. Introduction

The oxidation of alcohols to the corresponding carbonyl groups is a very useful reaction in both industrial and laboratory organic synthesis [1–3]. The resultant carbonyl-containing compounds are essential precursors or intermediates in the synthesis of various important substances such as pharmaceuticals, dyes, fragrances, industrially important chemicals, and natural products [1,2]. Because of the advantageous properties of hydrogen peroxide (H_2O_2), a number of useful procedures have been developed for H_2O_2-mediated oxidation of alcohols catalyzed by various ligand-complexed transition metal compound systems [3]. However, these homogeneous catalysts are often associated with disadvantages such as corrosion,

toxicity, handling, and difficulty in recovery and separation of the catalyst from reaction products [4]. Therefore, there has been considerable interest in the development of heterogeneous solid catalysts as promising substitutes for replacing these homogenous catalysts.

4-Hydroxy-2-butanone (HB) is currently used as an important intermediate for both pharmaceutical and food processing industries [5]. The present manufacture of HB is mainly based on the condensation of acetone with formaldehyde over sodium hydroxide solution at 40 °C [6]. The yields obtained reach up to 40–50% though large quantities of sodium hydroxide are consumed per batch. An alternative route to HB is the selective oxidation of 1,3-butanediol (1,3-BDO) [7]. It is shown that an attractive HB yield as high as 86% can be attained by using macroporous resin 2-methyl-4-poly (styrylmethyl) thiazolium hydrotribromide as stoichiometric oxidation reagents [7]. There is also usage of a homogeneous catalytic system based on Co/N-hydroxyphthalimide species for the aerobic oxidation of 1,3-BDO, which however can only

afford an unsatisfactory HB yield of ca. 50% [8]. Thus, from a practical point of view, it is highly attractive to develop user-friendly heterogeneous catalyst systems that can allow more efficient oxidation of 1,3-BDO to HB with oxygen or H_2O_2 under mild conditions.

In recent years, transition metal containing mesoporous materials have been emerging as promising easily recyclable catalysts for performing the selective oxidation reactions [9]. Of particular interest are the tungsten-containing mesoporous materials, which have been actively examined due to the fact that a large variety of tungsten-based homogeneous catalysts are known to display high activities in a number of useful oxidation procedures [10,11]. Along this line, much attention has been paid to the synthesis, characterization and catalytic properties of WO_x species anchored on various mesoporous silica systems [12–15]. Among the reactions investigated, the use of H_2O_2 as a "green" oxidant has been frequently examined and representative examples including epoxidation of alkenes, oxidation of sulfides, and oxidative cleavage of olefins [12–16].

Recently, we have reported that W-containing mesoporous materials are active solid catalysts for the oxidative cleavage of cyclopentene to glutaraldehyde with H_2O_2 in liquid phase, with the W-doped SBA-15 system is found to be the most efficient catalyst [12–15]. These catalysts are robust, purely inorganic materials resistant to oxidative degradation, in contrast to homogeneous tungsten-based catalysts. The aim of this work is to extend the investigation to the selective oxidation of 1,3-BDO to HB with H_2O_2 in liquid phase using the W-containing mesoporous materials. In view of the promising structural characteristics of mesocellular silica foams (MCF) materials which can provide more favorable conditions for mass transfer with respective to their more ordered counterparts SBA-15 or MCM-41 [17–21], in this study, a systematic investigation was attempted to prepare high quality W-containing MCF materials and used them as a new heterogeneous catalyst for the chosen reaction. The effect of tungsten loading and impact of the silica support structure on the performance of the W-containing materials have been discussed in the light of a detailed characterization of the physicochemical properties of the catalysts by N_2 adsorption, SAXS, XRD, TEM, DRIFTS, DR UV–vis and Raman.

2. Experimental

2.1. Catalyst preparation

The purely siliceous mesocellular silica foams (MCF) and W-doped MCF samples were prepared according to the direct hydrothermal method described in Ref. [22] using a Pluronic P123 triblock copolymer ($EO_{20}PO_{70}EO_{20}$, M_{av} = 5800, Aldrich) surfactant with 1,3,5-trimethylbenzene (TMB) as the organic swelling agent with TMB/P123 = 0.5 (w/w). In a typical preparation process, 5 g Pluronic P-123 triblock polymer, 2.5 g TMB and 28 g distilled water was added to 150 mL of HCl (2 M). The mixture was stirred for 4 h at 40 °C until it became homogeneous. Then 23 mL of tetraethyl orthosilicate (TEOS) in 20 mL ethanol and the required amount

of aqueous sodium tungstate solution ($NaWO_4 \cdot 2H_2O$, 0.2 M) were simultaneously and quickly added into the mixture under vigorous stirring. After 24 h at 40 °C, the milky reaction mixture is transferred to an autoclave and aged at 100 °C for another 24 h. The solid products were filtered off and dried overnight at 100 °C under static conditions. The occluded surfactant was removed by calcination at 600 °C for 5 h in air, yielding the final tungsten-containing mesoporous MCF material. For comparison, W-doped SBA-15 samples have been prepared by following the similar procedure as described above. Meanwhile, a W-impregnated MCF material (labeled as WO_3/MCF) has been prepared by an alcoholic impregnation method [23].

2.2. Catalyst characterization

Small-angle X-ray scattering (SAXS) experiments were performed on a Germany Bruker NanoSTAR U SAXS system equipped with high-resolution pinhole chamber using Cu Kα radiation (λ = 1.518 Å) and 106 cm sample to detector distance. The wide-angle X-ray powder diffraction (XRD) patterns were recorded on a Bruker D8 Advance spectrometer with Cu Kα radiation, which was operated at 40 mA and 40 kV. The specific surface area, pore volumes and the pore size distribution (PSD) of the samples were measured and calculated according to the BET method with a Micromeritics TriStar 3000 equipment with liquid nitrogen at 77 K. The method of Barret, Joyner, and Halenda (BJH) was used to determine the pore size distribution (PSD). Transmission electron micrographs (TEM) were obtained on a Joel JEM 2010 scan-transmission electron microscope. The samples were supported on carbon-coated copper grids for the experiment. The diffuse reflectance infrared Fourier transform spectroscopy (DRIFTS) measurements were performed using a Bruker Vector 22 instrument equipped with a DTGS detector and a Harrick diffuse reflectance cell equipped with ZnSe windows. Note that all DRIFT spectra were collected in dry air atmosphere at 200 °C. The laser Raman spectra were obtained on two separate confocal microprobe Jobin Yvon Lab Ram Infinity Raman systems equipped with excitation lines at 632.8 nm (He–Ne) and 325 nm (He–Cd), respectively. The tungsten content in W-doped MCF samples was determined by inductively coupled argon plasma (ICP, IRIS Intrepid, Thermo Elemental Company) after solubilization of the samples in HF:HCl solutions.

2.3. Activity test

The oxidation of 1,3-BDO (50 mmol) was carried out in the presence of o-hydroxyl phenol (0.25 mmol) as an auxiliary additive at temperature range from 35 to 80 °C under for 1–16 h using the tungsten-containing mesoporous silica catalysts (with tungsten amount corresponding to 1 mol% of substrate) with 50 wt.% aqueous H_2O_2 (100 mmol) as oxidant. The reaction products were analyzed by GC (Type GC-122, Shanghai) and the determination of different products in the reaction mixture was performed by means of GC–MS. There are four products
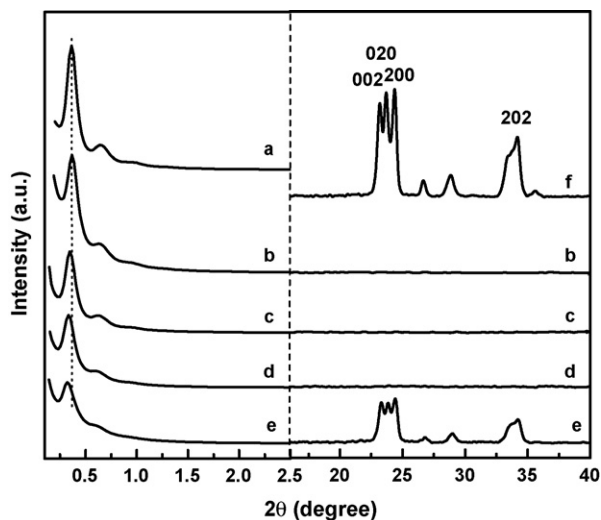
Fig. 1. SAXS (left) and wide-angle XRD (right) patterns of pure MCF (a), crystalline WO_3 (f), and W-MCF material with Si/W molar ratio of 40 (b), 30 (c), 20 (d) and 10 (e).

from the reaction: 4-hydroxy-2-butanone (HB), 2-hydroxy-4-butyl aldehyde (HA), acetate acid (AA) and formic acid (FA).

3. Results

3.1. Structural characteristics of the catalysts

The as-prepared tungsten-containing W-MCF samples have been analyzed using small-angle X-ray scattering (SAXS).

X-ray scattering is observed if uniformly sized particles are present, in contrast to X-ray diffraction associated with periodic structures [24]. The left panel to Fig. 1 shows the recorded SAXS data for the W-MCF samples with Si/W ratios ranging from 10 to 40. For the sake of comparison, the SAXS pattern of parent MCF is also included. As shown in Fig. 1a, the scattering pattern of the parent MCF material is well resolved and shows one strong primary peak and two higher order peaks with exponentially decreasing intensities. The occurrence of the higher order peaks is an indication of the narrow size distribution of the spherical cells [24]. Upon tungsten incorporation, a slight shift of the primary peak to a lower scattering angle was identified—for all W-MCF samples. This may result from a slight increase of the sphere diameters, possibly due to an expansion of their frameworks upon the incorporation of W heteroatoms [24]. In addition, a gradual attenuation in intensity of the primary peak was observed with increasing W loading. The consequence of such scattering reduction could be a partial structural collapse of the MCF pores as previously reported for high V-loaded MCF systems [23]. Moreover, for the as-synthesized W-MCF samples with Si/W molar ratios higher than 20, the absence of diffraction peaks at 2θ angles higher than $10°$ (Fig. 1b–d, right panel) indicates that the WO_x species can be well dispersed on the mesoporous MCF supports [14]. However, diffraction features corresponding to crystalline WO_3 were detected in the sample with a low Si/W molar ratio of 10.

Fig. 2 presents the TEM images of the W-containing MCF samples (including the parent MCF material), revealing that the characteristic three dimensional mesocellular arrangement of
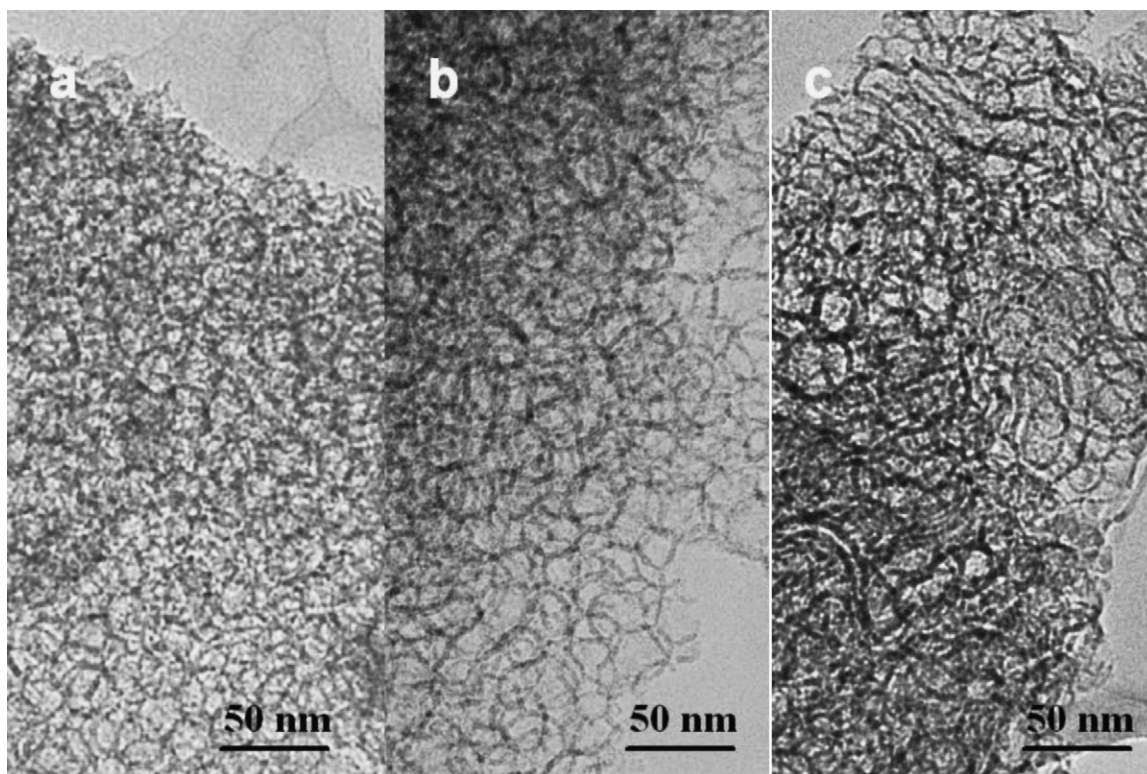

Fig. 2. Representative TEM images of (a) as-prepared parent MCF and the W-MCF samples with various Si/W ratios (b) W-MCF(20) and (c) W-MCF(10).

Table 1
Characteristics of the tungsten-containing mesoporous silica catalysts

Sample	Si/W[a] (mol)	Si/W[b] (mol)	S_{BET} ($m^2\,g^{-1}$)	V_p ($cm^3\,g^{-1}$)	D_C[c] (nm)	D_W[c] (nm)
Pure MCF	–	–	660	1.54	22.1	7.3
W-MCF(40)	40	48.1	652	1.38	22.3	6.4
W-MCF(30)	30	35.7	584	1.34	23.1	6.1
W-MCF(20)	20	21.5	557	1.22	23.6	5.6
W-MCF(10)	10	12.6	512	1.04	25.2	–
WO$_3$/MCF(20)	20	23.2	498	1.10	17.6	3.6
W-SBA-15(20)	20	24.3	669	1.06	6.5	–

[a] Stoichiometric ratio in gel.
[b] Measured by ICP-AES.
[c] Cell diameter, D_C, and window diameter, D_W, determined according to the BJH method.

the MCF frameworks could be largely retained after tungsten incorporation [18]. The cell sizes estimated from TEM are consistent with the cell sizes as determined from nitrogen sorption (D_C) summarized in Table 1. The wall thickness of the MCFs estimated by TEM is ∼4–6 nm, in agreement with the thick, robust framework walls observed in acid-synthesized MCF-type mesoporous silica as demonstrated in the literature [22]. Notice that a significant degradation in the mesocellular structure occurred for the W-MCF sample with Si/W ratio of 10, which is fully consistent with the results of the XRD studies thus further confirming that a Si/W ratio with up to 20 is favorable for maintaining the characteristic structural feature of the MCF materials.

The maintenance of the well-defined MCF frameworks upon tungsten introduction is further supported by the nitrogen sorption data. The nitrogen adsorption/desorption isotherms (not shown) are of type IV and show steep hysteresis of type H1 at high relative pressures. Inspection of the pore size distribution unambiguously further reveals that the 3D mesocellular structure of the MCF material has been primely preserved for the sample with Si/W ratio higher than 20. The specific surface area (S_{BET}) of the tungsten-containing samples is lower than that of the parent MCF material. The higher the tungsten content, the lower is the surface area. This decreasing trend is also shown by the data for the pore volumes. The results in Table 1 also clearly indicate that all W-MCF materials still possess pore volume and average pore sizes substantially larger than those of W-containing materials prepared by conventional impregnation or using mesoporous SBA-15 as the support. Thus, it can be concluded that the mesoporous MCF catalysts with a high pore volume and extremely large pore diameters (>22 nm) could be obtained at all W loadings in the present study. Obviously, all these structural and textural features may provide new attractive tungsten-containing catalyst systems possessing more favorable conditions in terms of mass transfer for catalytic applications [25–27].

DRIFT Spectroscopy in the skeletal region ranging from 1400 to 650 cm^{-1} has been employed to follow the variation behavior of the framework structure of the W-MCF samples as a function of tungsten loading. As shown in the spectrum of the parent MCF silica (Fig. 3a), the typical bands due to siliceous material Si–O–Si are observed: a main band at 1070 cm^{-1}, with a shoulder at 1200 cm^{-1}, due to asymmetric Si–O–Si stretching

modes as well as the corresponding symmetric stretch at 810 cm^{-1} [27]. Furthermore, in the spectra of the W-containing samples, an additional band at ca. 970 cm^{-1} is well developed for the samples with Si/W ratio up to 10. This observation is in good consistent with the recent results of the W-doped SBA-15 silica system reported by Dai and coworkers [14]. The band at around 970 cm^{-1} has been widely used to characterize the incorporation of transition metal atoms in the silica framework as the stretching Si–O vibration mode perturbed by the neighboring metal ions [28,29]. Thus, the presence of such an infrared band due to perturbed silica vibrations can be taken as an indication of the direct incorporation of the W atoms into the framework in the present W-MCF materials.

Laser Raman spectroscopy has been employed to elucidate the molecular nature of the tungsten species incorporated in the MCF materials. Fig. 4a shows the visible Raman spectrum of the pure siliceous MCF that exhibits spectroscopic features similar to amorphous SiO$_2$ [30]. Due to the presence of
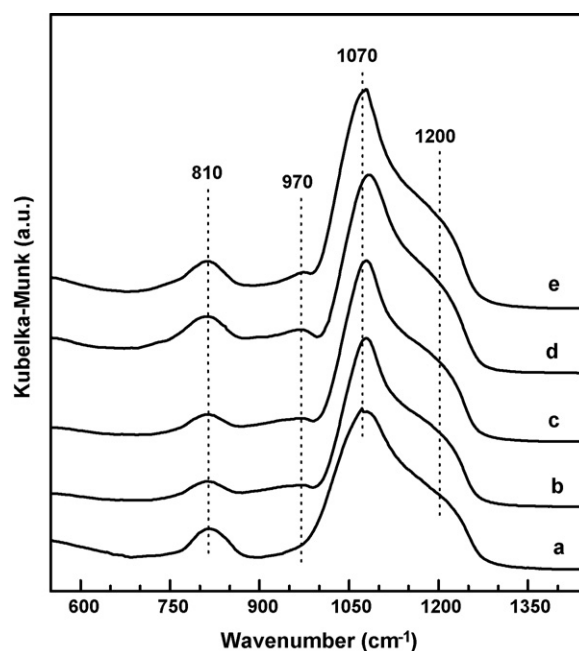

Fig. 3. FT-IR spectra of W-doped MCF catalysts with various Si/W ratios: (a) parent MCF; (b) W-MCF(40); (c) W-MCF(30); (d) W-MCF(20); (e) W-MCF(10).
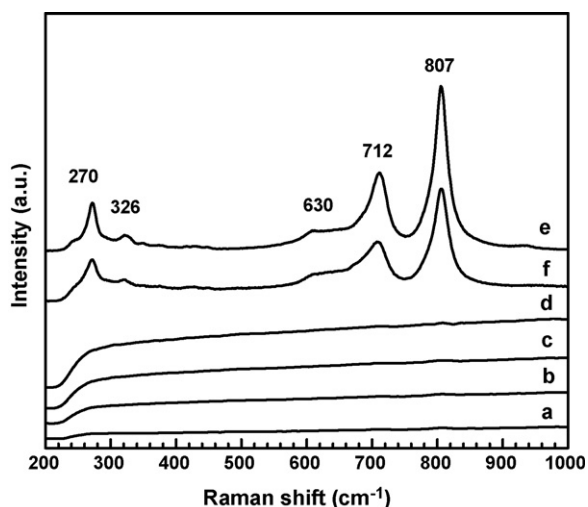
Fig. 4. Visible Raman spectra of the W-containing MCF catalysts: (a) parent MCF; (b) W-MCF(40); (c) W-MCF(30); (d) W-MCF(20); (e) W-MCF(10); (f) WO_3/MCF(20).

fluorescence interference and low sensitivity in the visible Raman experiments, the Raman intensity of the pure MCF silica is very weak. As shown in Fig. 4b–d, no Raman bands are observed for the W-MCF samples with Si/W ratio higher than 20, illustrating that the tungsten species in these samples are isolated or, at least, highly dispersed on the surface. When Si/W ratio in the sample is 10, four spectral features at ca. 807, 712, 326 and 270 cm^{-1} characteristic of crystalline WO_3 are clearly identified [31]. In combination with the TEM data, this demonstrates that, accompanied with the substantial structural degradation, the incorporation of excess amount of tungsten species would result in the undesirable formation of appreciable amount of nanocrystalline WO_3 on the surface of W-MCF materials. It is also clear that obvious Raman bands ascribed to crystalline WO_3 was detected for sample WO_3/MCF(20) obtained by conventional impregnation method, in contrast to the W-MCF(20) catalyst with the same Si/W ratio. This suggests that the direct hydrothermal method is more favorable for preparing W-containing MCF catalytic materials with a high dispersion of the tungsten oxide species at high tungsten loading levels.

The UV Raman spectra, as shown in Fig. 5, provide a further insight into the exact molecular structure of the present W-containing samples. In comparison with the visible Raman spectra as shown in Fig. 4, remarkably different spectral features are observed for all W-containing MCF samples. As shown in Fig. 5b–d, the Raman bands at 481, 500, 603, 661, 810, 905, and 976 cm^{-1} are observed for the low tungsten-containing W-MCF samples with Si/W ratio higher than 20. Band at 480 and 603 cm^{-1} is associated with the vibration of the siloxane rings of siliceous MCF [32]. The Raman bands at 905 cm^{-1} is characteristic of Si–O– and Si(–O–)$_2$ functionalities [33], which have been assigned to perturbed silica vibrations that are indicative of the formation of W–O–Si bonds [34]. The absence of the sharp bands at ca. 712 and 807 cm^{-1} characteristics of WO_3 in Fig. 5b–d further confirms that no crystalline WO_3 is formed in W-MCF samples with Si/W content higher than 20.
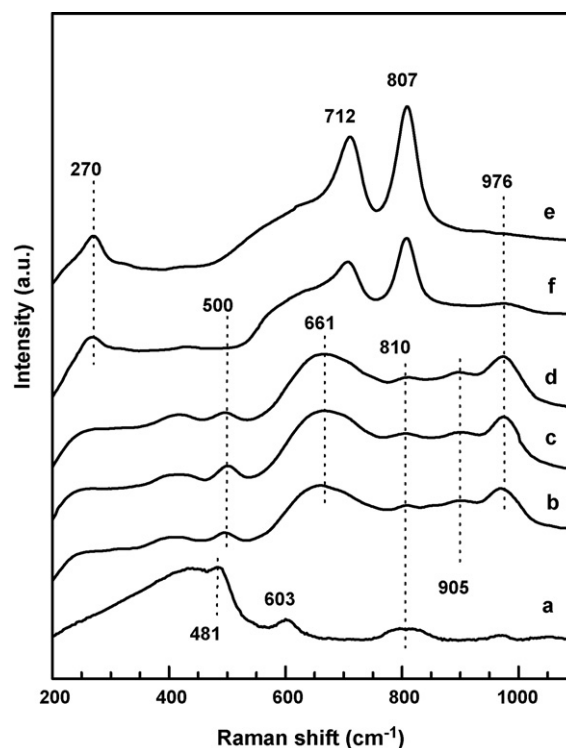

Fig. 5. UV Raman spectra of the W-containing MCF catalysts: (a) parent MCF; (b) W-MCF(40); (c) W-MCF(30); (d) W-MCF(20); (e) W-MCF(10); (f) WO_3/MCF(20).

Based on the literature assignment, the 976 cm^{-1} band is attributed to the symmetric stretching mode of the W=O bond of the isolated tetrahedral WO_4 species anchored on MCF [35]. The broad feature centered at 661 cm^{-1} can be assigned to stretching and bending modes of W–O bonds in the polymeric WO_x species, by comparison with previous results [36]. These results therefore suggest that the tungsten species in W-MCF samples with Si/W ratio higher than 20 are isolated or, at least, highly dispersed on the surface of the MCF materials [34].

Additional microstructural information on the surface WO_x species can be obtained from UV–vis diffuse reflectance measurements. The UV–vis DRS spectra of the various tungsten-containing MCF samples, as well as those of W-doped SBA-15 and bulk WO_3 are presented in Fig. 6. It is seen that the pure siliceous MCF displays no evident bands in the spectrum Fig. 6a, in agreement with previous studies on other mesoporous silica systems [36]. In the W-containing MCF samples, three absorption features centered at ca. 230, 290 and 440 nm were identified [34]. The broad band at about 440 nm registered for samples W-MCF(10), W-SBA-15(20) and WO_3/MCF(20) can be attributed to "bulk-like" WO_3 crystallites by comparing with the spectrum obtained in bulk WO_3 [15]. The other two main absorption features at 230 and 290 nm can be attributed to isolated W sites in tetrahedral coordination and polymeric W–O–W species, respectively [37]. The presence of these three bands has also been reported in tungsten oxide catalysts supported on MCM-48 or zirconia [38]. The absence of the strong absorption at 440 nm in Fig. 6b and c indicates that no crystalline WO_3 is formed in W-doped MCF samples when
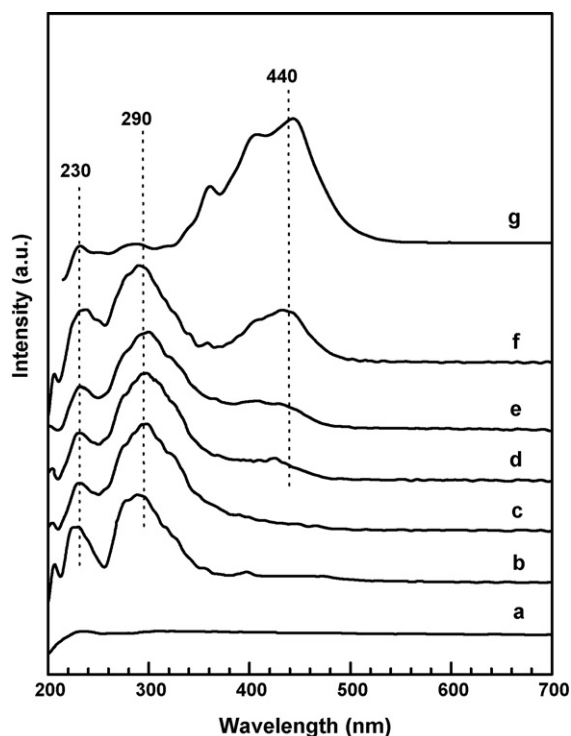
Fig. 6. UV–vis diffuse reflectance spectra of various samples after dehydration at 523 K in air for 2 h: (a) parent MCF; (b) W-MCF(30); (c) W-MCF(20); (d) W-SBA-15(20); (e) WO₃/MCF(20); (f) W-MCF(10); (g) bulk WO₃.

the Si/W ratio is higher than 20. Thus, the present UV–vis DRS spectra further demonstrates that a high dispersion of the tungsten oxide species is necessary for achieving the high catalytic performance in the W-containing mesoporous silica-based catalysts as discussed below.

3.2. Catalytic performance of different catalysts

The catalytic results obtained in the liquid-phase oxidation of 1,3-BDO at 65 °C over various supported mesoporous

tungsten oxide catalysts are shown in Table 2. 4-Hydroxy-2-butanone (HB), 2-hydroxy-4-butyl aldehyde (HA), acetate acid (AA) and formic acid (FA) were the main reaction products during the oxidation of 1,3-BDO on W-doped MCF catalysts (Table 2). The best catalyst in terms of HB formation is found to be the W-doped MCF sample with a Si/W molar ratio of 20. Under optimum reaction conditions, HB selectivity up to 78.1% at a high conversion of ca. 95.1% could be achieved over the catalyst W-MCF(20). It is also noticeable that the W-MCF(20) catalyst exhibited much higher BDO conversion and selectivity to HB than its homogeneous counterparts of H_2WO_4 catalyst. The lack of a higher selectivity toward HB production for the homogeneous catalysts is possibly due to the fact that the simple acids formation via the oxidative cleavage of 1,3-BDO or HB could be achieved much more efficiently over the H_2WO_4 catalyst [39]. At this point, it is also interesting to note that the reaction carried out in the absence of catalyst or auxiliary additive or with tungsten-free MCF showed much lower conversion (Table 2), thus confirming the role of tungsten ions in the reaction. All these activity results, in combination with the spectroscopic data as reported in Figs. 5 and 6, clearly demonstrate that the presence of the highly dispersed tungsten species incorporated in the silica matrix is necessary for the title reaction.

Moreover, as summarized in Table 2, the conversion of H_2O_2 is always higher than that of 1,3-BDO, indicating that H_2O_2 could not be efficiently used in the present reaction [14,15]. Indeed, it is found that H_2O_2 is partly decomposed into O_2 and H_2O as determined by volumetric measurement. Regarding the efficiency of H_2O_2, it appears that the higher the tungsten dispersion, the higher is the efficiency of H_2O_2 utilization. It is also clear from Table 2 that that the W-MCF(20) exhibited much higher 1,3-BDO conversion and selectivity to HB than those of mesoporous W-SBA-15(20), demonstrating that MCF is much superior to SBA-15 as a support. The high selectivity to HB on the former could be related to their highly isolated WO_x species dispersed on the mesocellular 3D structured MCF with

Table 2
Catalytic performance in the selective oxidation of 1,3-BDO over various samples[a]

Catalyst	H_2O_2 conv. (%)[b]	1,3-BDO conv. (%)	HB yield (%)	Selectivity (%)[c]			
				HB	HA	AA	FA
W-MCF(40)	91.2 (67.4)	83.4	43.8	52.5	2.2	24.6	20.7
W-MCF(30)	92.5 (65.1)	88.2	55.9	63.4	4.7	16.2	15.6
W-MCF(20)	93.1 (62.3)	95.1	74.3	78.1	6.8	7.9	7.2
W-MCF(20)[d]	15.5 (33.8)	8.0	5.5	69.0	27.3	2.3	1.4
W-MCF(10)	94.4 (56.4)	77.5	48.4	62.5	3.4	23.8	10.2
WO₃/MCF(20)	96.7 (60.3)	85.6	54.4	63.6	6.4	17.4	12.6
W-SBA-15(20)	95.6 (64.3)	89.3	55.6	62.3	3.4	18.1	16.2
H_2WO_4	84.2 (59.8)	72.6	44.4	61.2	4.1	21.3	16.4
MCF[e]	8.2 (49.1)	5.6	3.1	56.2	0.9	24.6	18.3
No catalyst	2.3 (47.3)	1.7	1.2	72.1	2.1	11.2	14.6

[a] Reaction conditions: 50 mmol 1,3-BDO; 7 mL 50% H_2O_2; 0.25 mmol o-hydroxyl phenol; $T = 65$ °C; reaction time 8 h; the reactions were carried out over the catalysts containing the same amounts of tungsten (tungsten amount = 1 mol% of substrate).

[b] H_2O_2 efficiency (data in parenthesis): the number of moles H_2O_2 consumed to produce the products/the number of moles H_2O_2 converted.

[c] HB, 4-hydroxy-2-butanone; HA, 2-hydroxy-4-butyl aldehyde; AA, acetate acid; FA, formic acid.

[d] Without o-hydroxyl phenol as an auxiliary additive.

[e] Tungsten-free parent MCF material.

an ultralarge pore diameter as described above. In a comparison of different preparative method for tungsten introduction, it is observed that the direct hydrothermal synthesis is more effective than the conventional impregnation method, as demonstrated by the higher activities and selectivities observed for W-MCF(20) with respect to those achieved on WO$_3$/MCF(20). Higher dispersion and isolation of the active species of W present on the direct hydrothermally synthesized W-MCF material can be attributed to the enhanced catalytic performance in the selective oxidation of 1,3-BDO to HB. Additionally, when comparisons among W-doped MCF series catalysts were taken, a much lower yield of HB is obtained for the sample with a Si/W ratio above or lower than 20, further confirming that the surface density and aggregation state of WO$_x$ species are also important for the selective oxidation of 1,3-BDO.

The catalytic activities of the W-MCF catalysts were also found to be strongly dependent on the reaction temperature. Fig. 7 shows the effect of reaction temperature on the selective oxidation of 1,3-BDO over catalyst W-MCF(20). In all cases, 4-hydroxy-2-butanone (HB) was obtained as the major product, and only small amounts of other products, viz., 2-hydroxy-4-butyl aldehyde (HA), acetate acid (AA), etc., were observed. At temperatures lower than 65 °C, the selectivity to HB was always high above 78% and the main side product was 2-hydroxy-4-butyl aldehyde (HA). Further, it can also be seen from the figure that the 1,3-BDO conversion increases with increase in reaction temperature, and that a maximum conversion was obtained at 65 °C. However, beyond this temperature, e.g., at 80 °C, a decrease in conversion and selectivity to main product of HB was observed, which could be attributed to a possible decomposition of H$_2$O$_2$ [9].

To gain a further insight into the effect of reaction time on the catalytic behaviour of the W-MCF(20) catalyst, the conversion and product selectivity for the selective oxidation of 1,3-BDO was studied at a constant reaction temperature of 65 °C as shown in Fig. 8. It can be seen from this figure that the

Fig. 8. Influence of reaction time on the conversion of 1,3-BDO and selectivity of all the products over catalyst W-MCF(20). Experimental conditions: 50 mmol of 1,3-BDO, 7 mL of 50 wt.% H$_2$O$_2$ and 0.25 mmol o-hydroxyl phenol; tungsten amount = 1 mol% of substrate; reaction at 65 °C.

(1,3-BDO) conversion increases with time, while (4-hydroxy-2-butanone, HB) selectivity decreases, and that the optimum conversion and selectivity could be achieved at about 8 h. It can also be noticed from this figure that, at the initial stages, a small amount of acetate acid and formic acid was observed along with 2-hydroxy-4-butyl aldehyde (HA). The fact that no appreciable variation in the selectivity for HA formation was observed when the reaction time is longer than 8 h implies that the overoxidation pathway may proceed mainly through the consecutive oxidative cleavage of HB. These results show that the proper choice of reaction time is also very crucial for obtaining good conversion and HB formation.

The activity in 1,3-BDO oxidation obtained on the W-MCF(20) catalyst after different reuses is presented in Table 3. It is remarkable that the W-MCF(20) sample maintained its high catalytic activity affording a high HB yield above 60% even after four recyclings and reuse of the catalyst (entries 1–4 in Table 3). On the other hand, the WO$_3$/MCF(20) catalyst exhibiting a moderate activity during the first cycle experience a strong and continuous deactivation during the second and third cycle of test. The observed results clearly evidenced the high efficiency and selectivity of the present direct hydro-thermal method to incorporate tungsten into the silica framework without formation of the extra-framework WO$_3$ which was progressively leached out towards the solution resulting in a gradual loss of catalytic activity as a function of cycling tests.

In order to examine the possible catalytic activity due to leached metal ions, in a separate experiment, the reaction mixture was filtered after 2 h under hot conditions and the experiment was continued in the filtered solution without any solid catalyst of W-MCF(20) after adding new reactants. No further 1,3-BDO conversion was observed, thus indicating that homogeneous catalysis is not taking place under the reaction conditions. Moreover, based on the elemental results followed by ICP-AES analysis, there is no detectable leaching of W-species or apparent loss of tungsten could be evidenced in the
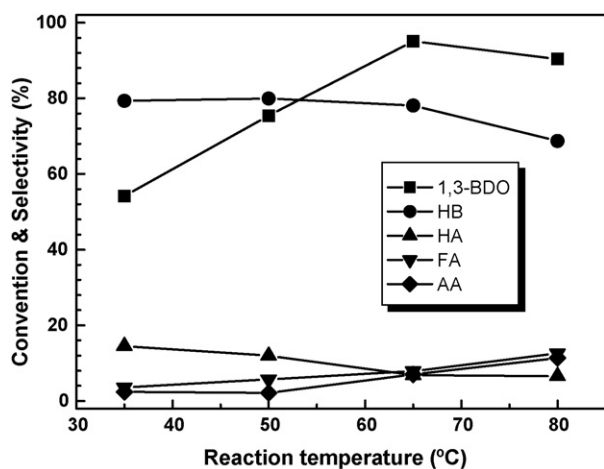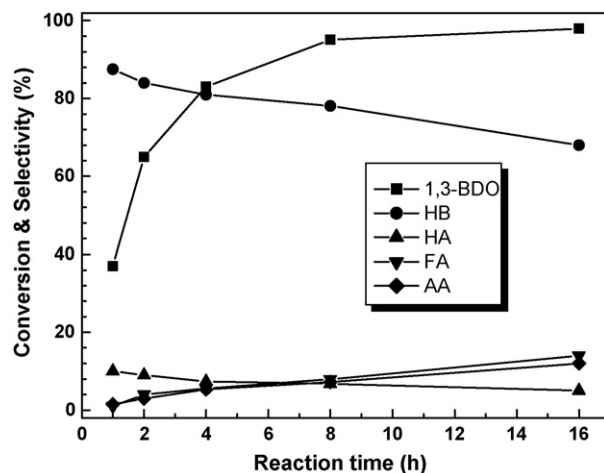

Fig. 7. Influence of reaction temperature on the conversion of 1,3-BDO and selectivity of all the products over catalyst W-MCF(20). Experimental conditions: 50 mmol of 1,3-BDO, 7 mL of 50 wt.% H$_2$O$_2$ and 0.25 mmol o-hydroxyl phenol; tungsten amount = 1 mol% of substrate; reaction for 8 h.

Table 3
Reusability of the W-MCF(20) and WO₃/MCF catalyst[a]

Catalyst	Entry	H_2O_2 conv. (%)	1,3-BDO conv. (%)	HB yield (%)	Selectivity (%)[b]			
					HB	HA	AA	FA
W-MCF(20)	1	93.1	95.1	74.3	78.1	6.8	7.9	7.2
	2	93.4	93.7	72.3	77.2	7.2	7.2	8.4
	3	91.2	91.0	68.7	75.5	8.3	7.2	9.0
	4	92.8	92.4	68.2	73.8	8.7	8.3	9.2
WO₃/MCF(20)	1	96.7	85.6	54.4	63.6	6.4	17.4	12.6
	2	86.1	73.2	43.1	58.9	8.7	18.6	13.8
	3	80.4	68.5	38.1	55.6	6.4	20.6	17.4
	4	74.3	65.5	34.5	52.7	7.6	21.2	18.5

[a] Reaction conditions: 50 mmol 1,3-BDO; 100 mmol 50% H_2O_2; $T = 65\ °C$; reaction time 8 h; tungsten amount = 1 mol% of substrate.
[b] HB, 4-hydroxy-2-butanone; HA, 2-hydroxy-4-butyl aldehyde; AA, acetate acid; FA, formic acid.

W-MCF(20) samples, indicating the presence of strong interaction between tungsten species and the silica-based MCF matrix structure.

4. Discussion

Featuring with an open porosity and ultralarge pore size, mesocellular silica foams (MCF) have attracted great recent attention as new promising adsorption and catalytic materials owing to their highly accessible and open porosity by providing more favorable conditions for mass transfer compared to their conventional mesoporous counterparts [20,40]. A recent work by Kaliaguine and coworkers has described the use of MCF materials as an excellent support for preparation of a new type of TS-1 zeolite coated mesoporous materials, which exhibited a high specific activity in the liquid-phase selective hydroxylation of a bulky molecule 1-naphthol as compared to conventional TS-1 counterparts [25]. More recently, we have reported that the use of mesoporous MCF silica as a support can allow the generation of a new type of highly efficient V-containing MCF catalyst system in the gas phase oxidative dehydrogenation (ODH) of propane to propylene [23]. In this work a new transition metal containing mesoporous catalyst system W-MCF featuring highly accessible and opening mesoporosity as active and recyclable catalysts for the liquid-phase oxidation of 1,3-butanediol to 4-hydroxy-2-butanone (HB) in the presence of H_2O_2 has been demonstrated. The present results show that the tungsten-containing MCF catalyst obtained by a direct hydrothermal synthesis is highly effective for the selective conversion of 1,3-BDO to HB in the H_2O_2 system, offering HB yields much higher than conventional tungsten-based catalysts.

Characterization by means of UV–vis DRS and UV Raman has proved that, at low tungsten oxide contents (Si/W ratio higher than 20), the surface of the W-MCF samples is mainly covered by isolated tungsten or low polymeric tungsten species, which are well incorporated into the framework of MCF materials. These highly dispersed WO_x species may be responsible for the superior performance of the catalysts in the selective oxidation of 1,3-BDO. At a higher tungsten content (Si/W ratio ∼ 10), crystalline tungsten trioxide

appeared on the surface of the sample and a significant degradation of the mesocellular arrangement of MCF pores occurred, leading to the decrease in the catalytic activity. Moreover, it is worth noting that the W-MCF(20) catalyst showed superior activity as compared to its hexagonally ordered counterpart, i.e., W-doped SBA-15. Such superiority could, however, be directly related to the higher dispersion of the tungsten oxide species as evidenced for catalyst W-MCF(20) with respect to W-SBA-15(20). The fact that a higher amount of isolated or low polymeric tungsten species is achievable in the MCF matrix as compared to the SBA-15 silica may be a consequence of the presence of a higher OH surface concentration in the MCF material [23].

On the other hand, when comparisons among W-doped MCF series catalysts were taken, the W-MCF(20) material with a Si/W ratio of 20 showed the best catalytic performance. This indicates that both isolated and low polymeric tungsten species are active and selective for 1,3-BDO conversion. More careful inspections of the activity and characterization results reveal that in addition to the aggregation state, the surface density and in particular the distance between active WO_x sites are also important parameters that have to be considered in order to account for the observed catalytic behavior in the selective oxidation of 1,3-BDO [23]. It is also interesting to note that the addition of o-hydroxy-phenol as an auxiliary additive in the present reaction system appears to be another key factor influencing the 1,3-BDO oxidation with the W-MCF materials. As shown in Table 2, the absence of o-hydroxyl phenol strongly diminishes the oxidation of 1,3-BDO with the W-MCF(20) material. In the case of the liquid-phase oxidation reactions mediated by transition metal homogeneous or heterogeneous catalysts, a radical or an ionic reaction mechanism has been proposed when working with H_2O_2 as oxidant, respectively [41]. Taking into account that the presence of excess amount of o-hydroxyl phenol as an radical inhibitor is beneficial for the 1,3-BDO oxidation on W-MCF catalyst, it appears reasonable to think that the reaction may proceed through a nonradical mechanism and the main role of the o-hydroxy-phenol is to suppress the unproductive decomposition of the oxidizing agents. Nevertheless, these results are not conclusive and further research is needed to confirm the oxidation pathway.

Compared to the visible Raman spectra as reported in Fig. 4, the UV Raman spectra of the W-MCF samples as shown in Fig. 5 display significant differences in the 500–1050 cm^{-1} range. The well-defined Raman band at 976 cm^{-1} associated with the terminal W=O stretches of isolated tetrahedral WO$_4$ species in present UV Raman spectra has also not been identified in the visible Raman spectra for other W-containing mesoporous materials, such as W-SBA-15 and W-MCM-48 [14,15]. A number of recent studies concerning the use of UV Raman as a powerful technique for structural elucidation of highly dispersed transition metal species has shown that the resonance Raman effect may provide unique opportunity to identify the exact molecular structure of the isolated metal oxide species imbedded in the mesoporous or nanoporous matrix, especially at the case when the metal loading is very low [42–44]. In the present work, it is likely that the W=O band corresponding to the highly isolated WO$_4$ species could be preferentially resonance enhanced by the 325-nm line excitation, thus leading to the appearance of well-defined band characteristic of the W=O bond at ca. 976 cm^{-1}. Therefore, the present UV Raman band with vibrational frequency at 976 cm^{-1} corresponding to W=O stretches provides direct spectroscopic evidence for the presence of highly isolated tungsten oxide species with tetrahedral structure in the low tungsten-containing W-MCF materials.

It is also well documented that heterogenized homogeneous catalyst systems often suffer from extensive leaching of active metal species during reactions and eventually lose their catalytic activity [45]. In the present work, the high stability of the W-MCF(20) catalyst towards deactivation was attributed to the high interaction between the W species and the MCF surface, which strongly reduces tungsten leaching during the repeated tests and clearly prevents from the presence of any bulk WO$_3$ species. The observed results clearly evidenced the high efficiency and selectivity of the direct hydrothermal method to incorporate tungsten into the silica framework without formation of the extra-framework WO$_3$ which was progressively leached out towards the solution resulting in a gradual loss of catalytic activity as a function of cycling tests. Indeed, if most of tungsten was presented in the form of WO$_3$ as evidenced for WO$_3$/MCF(20) sample, it would be rapidly dissolved away by the hydrogen peroxide leading to the formation of the soluble tungsten peroxo species and thus, a rapid deactivation was observed on the second run as very small amount of tungsten was remained on the mesoporous silica framework. It follows, that the activity is clearly due to W-species, whatever their aggregation state, but to perform several catalytic cycles, one needs to have anchored species on the surface.

5. Conclusions

In summary, high-quality mesoporous W-MCF materials featuring a well-defined three dimensional (3D) mesoporosity and ultralarge mesopores with different Si-to-W ratios were successfully synthesized using a direct hydrothermal method. Characterization by means of DRIFTS, TEM, DR UV–vis and Raman spectroscopy show that a high tungsten content up to 20 wt.% could be well incorporated into the framework of the MCF material. The W-doped MCF materials appear to be suitable for an use as catalyst in selective oxidation of 1,3-BDO to HB in the hydrogen peroxide system. The catalyst exhibits a high activity and an extremely high stability as a function of the test and reuse due to the presence of three dimensional mesocellular network with ultralarge mesopores which favors the diffusion of reactants and products. Work is on going to test the W-MCF material in other reactions where the highly accessible and uniform open mesoporosity as well as the high specific surface area could be useful.

References

[1] R.A. Sheldon, J.K. Kochi, Metal-catalyzed Oxidation of Organic Compounds, Academic Press, New York, 1981.
[2] A. Proto, C. Capacchione, A. Scettri, O. Motta, Appl. Catal. A 247 (2003) 75.
[3] W.P. Griffith, J.M. Joliffe, Dioxygen Activation and Homogeneous Catalytic Oxidation, Elsevier, Amsterdam, 1991.
[4] R.A. Sheldon, I.W.C.E. Arends, A. Dijksman, Catal. Today 57 (2000) 157.
[5] N. Ichikawa, S. Sato, R. Takahashi, T. Sodesawa, Catal. Commun. 6 (2005) 19.
[6] T. Ogura, T. Maeda, M. Nagao, T. Takesawa, T. Ishizaki, Takasago Perfumery Co., Ltd., Japan, Kokai Tokkyo Koho, JP Patent (2004) 210,650.
[7] A. Kessat, A. Babadjamian, A. Iraqi, Eur. Polym. J. 37 (2001) 131.
[8] T. Iwahama, T. Yoshino, T. Keitoku, S. Sakaguchi, Y. Ishii, J. Org. Chem. 65 (2000) 6502.
[9] N. Srinivas, V.R. Rani, M.R. Kishan, S.J. Kulkarni, K.V. Raghavan, J. Mol. Catal. A: Chem. 172 (2001) 187.
[10] J.F. Deng, X.H. Xu, H.Y. Chen, A.R. Jiang, Tetrahedron 48 (1992) 3503.
[11] H. Furukawa, T. Nakamura, H. Inagaki, E. Nishikawa, C. Imai, M. Misono, Chem. Lett. 5 (1988) 877.
[12] H. Chen, W.L. Dai, J.F. Deng, K.N. Fan, Catal. Lett. 81 (2002) 131.
[13] X.L. Yang, W.L. Dai, H. Chen, Y. Cao, H.X. Li, H.Y. He, K.N. Fan, J. Catal. 229 (2005) 259.
[14] X.L. Yang, W.L. Dai, H. Chen, J.H. Xu, Y. Cao, H.X. Li, K.N. Fan, Appl. Catal. A 283 (2005) 1.
[15] X.L. Yang, W.L. Dai, R.H. Gao, H. Chen, H.X. Li, Y. Cao, K.N. Fan, J. Mol. Catal. A: Chem. 241 (2005) 205.
[16] D.H. Koo, M. Kim, S. Chang, Org. Lett. 7 (2005) 5015.
[17] F. Somma, G. Strukul, J. Catal. 227 (2004) 344.
[18] P. Schmidt-Winkel, W.W. Lukens Jr., D. Zhao, P. Yang, B.F. Chmelka, G.D. Stucky, J. Am. Chem. Soc. 121 (1999) 254.
[19] J.S. Lettow, Y.J. Han, P. Schmidt-Winkel, P. Yang, D. Zhao, G.D. Stucky, J.Y. Ying, Langmuir 16 (2000) 8291.
[20] D.T. On, S. Kaliaguine, J. Am. Chem. Soc. 125 (2003) 618.
[21] P. Wu, T. Tatsumi, T. Komatsu, T. Yashima, J. Catal. 202 (2001) 245.
[22] P. Schmidt-Winkel, W.W. Lukens Jr., P. Yang, D.I. Margolese, J.S. Lettow, J.Y. Ying, G.D. Stucky, Chem. Mater. 12 (2000) 686.
[23] Y.M. Liu, W.L. Feng, T.C. Li, H.Y. He, W.L. Dai, W. Huang, Y. Cao, K.N. Fan, J. Catal. 239 (2006) 125.

[24] L.A. Feigin, D.I. Svergun, Structure Analysis by Small-angle X-ray and Neutron Scattering, Plenum, New York, 1987.

[25] D.T. On, A. Ungureanu, S. Kaliaguine, Phys. Chem. Chem. Phys. 5 (2003) 3534.

[26] A. Ungureanu, D.T. On, E. Dumitriu, S. Kaliaguine, Appl. Catal. A 254 (2003) 203.

[27] P. Kústrowski, L. Chmielarz, R. Dziembaj, P. Cool, E.F. Vansant, J. Phys. Chem. B 109 (2005) 11552.

[28] P. Shaha, A.V. Ramaswamy, K. Lazarc, V. Ramaswamya, Appl. Catal. A 273 (2004) 239.

[29] P. Wu, T. Tatsumi, T. Komatsu, T. Yashima, J. Catal. 202 (2001) 245.

[30] J.G. Graselli, B.J. Bulkin, Analytical Raman Spectroscopy, Wiley, New York, 1991, pp. 352–353.

[31] J.M. Brégeault, J.Y. Piquemal, E. Briot, E. Dupery, F. Launay, L. Salles, M. Vennat, A.P. Legrand, Microporous Mesoporous Mater. 44–45 (2001) 409.

[32] K.J. Chao, C.N. Wu, H. Chang, L.J. Lee, S.F. Hu, J. Phys. Chem. B 101 (1997) 6341.

[33] P. McMillan, Am. Mineral. 69 (1986) 622.

[34] X. Gao, S.R. Bare, B. Weckhuysen, I.E. Wachs, J. Phys. Chem. B 102 (1998) 10842.

[35] E. Duprey, P. Beaunier, M.-A. Springuel-Huet, F. Bozon-Verduraz, J. Fraissard, J.-M. Manoli, J.-M. Brégeault, J. Catal. 165 (1997) 22.

[36] J.Y. Piquemal, E. Briot, M. Vennat, J.-M. Brégeault, G. Chottardb, J.-M. Manolic, Chem. Commun. 1195 (1999).

[37] E. Briot, J.-Y. Piquemat, M. Vennat, J.-M. Brégeault, G. Chottard, J.-M. Manoli, J. Mater. Chem. 10 (2000) 953.

[38] J.C. Vartuli, J.G. Santiesteban, P. Traverso, N. Cardona-Martinéz, C.D. Chang, S.A. Stevenson, J. Catal. 187 (1999) 131.

[39] V. Carlo, R. Marco, J. Org. Chem. 51 (1986) 1599.

[40] Y.J. Han, J.T. Watson, G.D. Stucky, A. Butler, J. Mol. Catal. B 17 (2002) 1.

[41] O. Bortolini, V. Conte, F. Di Furia, G. Modena, J. Org. Chem. 51 (1986) 2661.

[42] P.C. Stair, C. Li, J. Vac. Sci. Technol. A 15 (1997) 1679.

[43] C. Li, G. Xiong, Q. Xin, J. Liu, P. Ying, Z. Feng, J. Li, W. Yang, Y. Wang, G. Wang, X. Liu, M. Lin, X. Wang, E. Min, Angew. Chem. Int. Ed. Eng. 38 (1999) 2220.

[44] Y.T. Chua, P.C. Stair, I.E. Wachs, J. Phys. Chem. B 105 (2001) 8600.

[45] Y. Cao, J.C. Hu, P. Yang, W.L. Dai, K.N. Fan, Chem. Commun. (2003) 908.